LU TP 04 - 21
May, 2004

Studies of Boson Gluon Fusion Events in Deep Inelastic e-p Scattering

Master of Science Thesis by Tobias Toll

Thesis advised by Gösta Gustafson

Department of Theoretical Physics,
Lund University, Lund, Sweden

Abstract

There are many models describing DIS-events. For many observables the Colour Dipole Model, as implemented in ARIADNE, gives the best description. Compared to other models the CDM contains many elements which cannot be derived from perturbative QCD. To further understand the strong force it is therefore interesting to compare the CDM to other models. In this thesis a new version of ARIADNE is introduced in which BGF events are treated in a way which is different from the default version. Two effects have been investigated: the correlation between seaquarks at BGF events, and the correlations of the emissions from the two colour-lines of the struck gluon. For the first effect, comparisons to experimental data obtained at HERA by the H1 Collaboration were made. A clear signal between the two versions was found but the differences were too small in the kinematic region where H1 perform measurements, for any definite conclusions to be drawn. A strong signal was also found in the correlation between emissions from the two colour-lines of the struck gluon. More experimental results for comparisons would be welcome!

Contents

1 Introduction

The important thing is not to stop questioning.
Curiosity has its own reason for existing.
Albert Einstein

Out of curiosity, 39 institutes from 12 countries, together built a huge device called HERA, at the physics facility DESY in Hamburg, Germany. In HERA protons and electrons are made to collide at high energies. In such collisions the initial protons disintegrate and what is observed is large amounts of hadrons. In order to obtain a theoretical description of these events the fundamental theory is too complicated and can therefore not be used for a complete description. Instead different models are used to make predictions and help us understand what takes place in the experiments, somewhat appeasing our curiosity. This thesis is a contribution, however small, to one such model and hence to our further understanding of nature.

The high energy process at HERA can be divided into two phases as shown in fig. 1. The first phase is a perturbative phase where all the particles involved are very close to each other. This phase is thus dominated by large momentum transfers. Constituents of the hadrons are created in the perturbative phase but no hadrons. When the particles get more separated, they enter into a phase dominated by soft interactions, where the hadrons are formed.

In this thesis two models, one for each phase, have been used to simulate HERA events. For the perturbative phase the Colour Dipole Model (CDM), implemented in the Monte Carlo ARIADNE[2], has been used as described in section 3. For the hadronization phase the Lund String Model[1], described in section 2.6, has been used as implemented by the program PYTHIA[7].

There are many models describing the events taking place at HERA. Such models take their motivation from perturbative Quantum Chromo Dynamics, abbreviated QCD, the fundamental theory described briefly in section 2.2. For many observables it turns out that the Colour Dipole model gives the best description. CDM contains more elements which cannot be derived from perturbative QCD however. Therefore it is interesting to look at the connection between CDM and other models, and hence see if CDM may be better motivated in order for us to enhance our understanding about the strong force.

The purpose of this thesis is to implement changes in ARIADNE motivated by QCD and other models such as Mueller's dipole model [5] described in section 3.6, and to see what effect this has on the results from the program. The changes concern a special kind of events called Boson Gluon Fusion, described in section 3.4. I have compared the new version of ARIADNE, containing the changes, to the old version. I have been looking at two effects. The first is the correlation between seaquarks and the second effect concerns the correlation between the $p_\perp$ of the emissions in the two versions of ARIADNE. In the first case I have also made comparisons to experimental results from HERA.

This thesis consists of three parts. In section 2 an overview of the underlying models and concepts is given. This section may be skipped by the initiated reader. In section 3 the Colour Dipole Model and the ARIADNE cascade is described. This section also includes a subsection about Mueller's dipole model[5], which is a formulation of the parton cascade with transverse space coordinates instead of momentum. Some of the implications of Mueller's formulation further motivates this thesis as described there.

Section 4 describes what I have done and the results obtained. There the changes made in ARIADNE and the expected differences between the two versions are described.

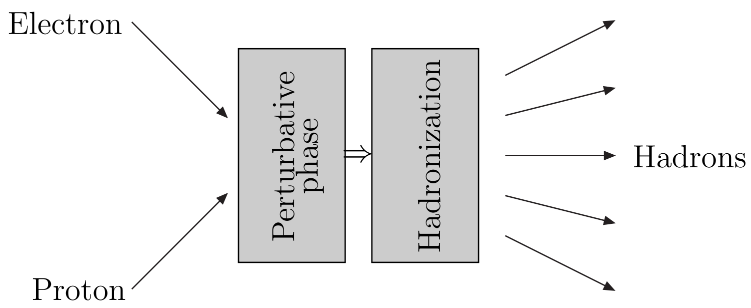

Figure 1: When an electron and a proton collide at HERA, many hadrons are created. The intermediate states may be divided into a perturbative phase and a soft hadronization phase.

In section 4.1 the two versions of ARIADNE are then compared to each other and to experimental data collected at HERA, concerning correlations between heavy quarks. In section 4.2 the two versions are compared regarding correlations between transverse momenta of the emitted hadrons. In this section some suggestions for future experiments are made. Such experiments would be welcome in order for us to determine how the Colour Dipole Model should be further developed and better understood, helping us in our description of the strong force.

Enjoy the thesis!

2 Overview and Background

2.1 The Standard Model of Particle Physics

The not very imaginative name of the theory describing all the fundamental building blocks of matter and how they interact is: The Standard Model of Particle Physics. It concerns us because it describes electrons and the quarks building up protons and neutrons which together with the electrons form atoms building up the molecules we are made of.

The fundamental particles can be divided into two main groups: the Fermions including all the spin-1/2 particles building up all matter, and the Bosons including all the spin-1 particles responsible for the interactions between the fermions.

The interactions originates from gauge symmetries of the Standard Model. Those are included into the Lagrangian density of the Standard Model which governs the dynamics of the fermions and bosons. In the standard model there are three gauge symmetries. Those are the $SU(3)$ symmetry of all strongly interacting particles and the $SU(2)$ symmetry which combined with the $U(1)$ symmetry gives the electroweak force. The fermions may be presented in $SU(2)$ doublets as

$$
\begin{array}{lccccc}
 & & & & \begin{array}{c} Charge \end{array} \\
\text{Quarks :} & \begin{pmatrix} u \\ d \end{pmatrix} & \begin{pmatrix} c \\ s \end{pmatrix} & \begin{pmatrix} t \\ b \end{pmatrix} & \begin{array}{c} +2/3 \\ -1/3 \end{array} \\
\text{Leptons :} & \begin{pmatrix} \nu_e \\ e \end{pmatrix} & \begin{pmatrix} \nu_\mu \\ \mu \end{pmatrix} & \begin{pmatrix} \nu_\tau \\ \tau \end{pmatrix} & \begin{array}{c} 0 \\ -1 \end{array}
\end{array}
$$

Here one column represents a "family". Our world is built up entirely by the particles of the first family, e, ν_e, d and u. The particles in the other families have the same properties as the ones in the first family, the only difference being they are heavier. This makes them unstable, and they will all decay into particles of the first family. The quarks may also be put into $SU(3)$ triplets, for example

$$\begin{pmatrix} u_r \\ u_g \\ u_b \end{pmatrix} . \tag{1}$$

The indices r, g and b are called colour-indices and denote red, green and blue respectively. The colour is the charge of the strong force. We never see any free quarks or coloured objects, only antisymmetric combinations of the colours into colourless states. In the picture of the doublets and triplets the gauge bosons play the role of transforming a particle within the doublet or triplet into another one as in fig. 2.

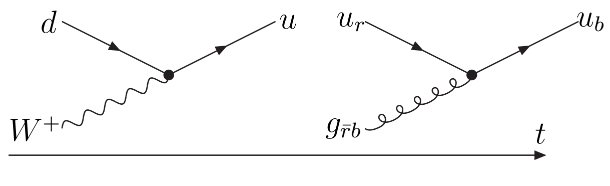

Figure 2: The gauge bosons transform a particle into another within a group. In $SU(2)$ the W-bosons therefore have to be charged, and in $SU(3)$ the gluons need to carry a colour and an anticolour.

The gauge bosons transforming the fermions in $SU(2)$ are called $W^{\pm}$. For electric charge to be conserved in the transformation they need to be charged as the superscripts indicate. The mediators of the strong force of $SU(3)$ are called gluons because they seem to glue matter very strongly together. For colour to be conserved in $SU(3)$-transformations the gluons themselves need to carry colour. The implications of this will be further described in section 2.6. Apart from the $W^{\pm}$-bosons, the $SU(2)$ symmetry also contains a neutral boson W^0 which does not transform the fermions into each other. The $W^{\pm}$ and W^0 can in turn be put into an $SU(2)$ triplet, and the gluons can be put into an $SU(3)$ octet. The boson of the $U(1)$ symmetry is called B.

The W^0 of $SU(2)$ and the B-boson of $U(1)$ are not energy eigenstates in the Standard Model. Instead two certain linear combinations of W^0 and the B-boson are eigenstates to the energy. One such combination is the photon γ and the other is the Z^0-boson.

In this thesis I have looked solely upon collisions between electrons and protons. The structure of the latter is described is section 2.3.

2.2 Quantum Chromo Dynamics (QCD)

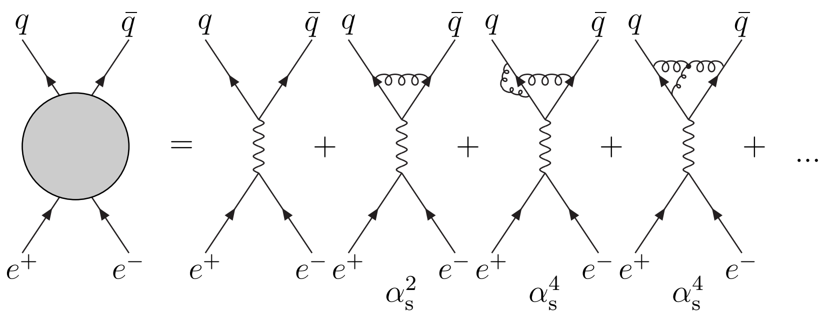

Figure 3: An event including the strong force may be written as a sum of events in ascending order in α_s in perturbative QCD.

The theory describing the interactions between the coloured quarks and gluons is called Quantum Chromo Dynamics or QCD. The probability for obtaining a particular result in an event involving quarks and gluons is difficult to calculate exactly from the fundamental theory. Instead a perturbative approach is often used. The idea is that to obtain a specific final state from a specific initial state all the possible states in between interfere with each other. The amplitudes, or matrix elements, for all possible intermediate states must then be added before the probability for the event can be calculated.

In perturbative QCD the amplitude is expanded in powers of the strong coupling constant α_s, as visualized in fig. 3. For an exact calculation all orders in α_s are needed. The perturbative QCD approach demands the coupling α_s to be small. This is not always the case, because α_s depends on the momentum transfer at the vertices. At small momentum transfers α_s becomes large and the expansion is no longer useful. Non-perturbative models are then needed to describe the event. One such model is the Lund String Model described in section 2.6.

2.3 The Parton Model

In 1968 physicists proved experimentally, in electron-proton scattering, that the proton consists of many point-like particles. These have been given the common name partons.

Three particles, two up-quarks and one down-quark, giving the proton its electric charge, are called valence quarks by spectroscopic analogies. The proton also contains particles not contributing to its charge. The quarks are bound together by the strong force mediated by gluons, and there is no physical reason for these gluons not to split up into virtual quark-antiquark pairs called sea-quarks, which they do. Since gluons also carry colour they can themselves emit even more gluons. The gluons carry about half the momentum of the proton.

2.4 Deep Inelastic Scattering (DIS)

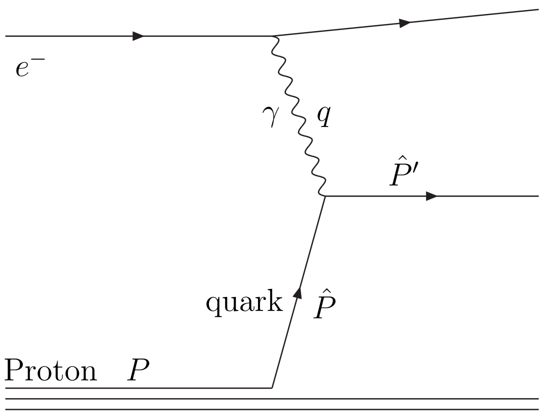

Figure 4: A Deep Inelastic Scattering between an electron and a proton.

In fig. 4 we see a diagram of a typical electron proton scattering event. The scattering is mediated by a virtual photon with virtuality $Q^2 \equiv -q^2$. The scattering in fig. 4 is deeply inelastic in the sense that the total mass of the outgoing hadrons is much larger than the mass of the incoming proton. The sub-scattering between the electron and the quark is elastic, however. The four-momentum of the struck quark is $\hat{P} = xP$, i.e. it carries a fraction x of the four-momentum of the proton. Conservation of four-momentum in the sub-collision yields $1 = Q^2/2\hat{P}q$ or, from the definition of $\hat{P}$:

$$x = x_{Bj} = \frac{Q^2}{2Pq}. \tag{2}$$

This defines the Bjorken x-variable.

2.5 Structure Functions

When a photon interacts with a proton the interaction is given by the sum of interactions with the partons in the proton. We define a probability distribution $f_i(x)$ as the probability that a parton of type i carries four-momentum fraction x. The total cross-section for the photon-proton scattering is given by $\sigma_{\gamma^* p} \sim \frac{\alpha}{Q^2} F_2$, where the interaction with the photon is determined by a combination of probabilities according to

$$F_2(x) = \sum_i e_i^2 x f_i(x), \tag{3}$$

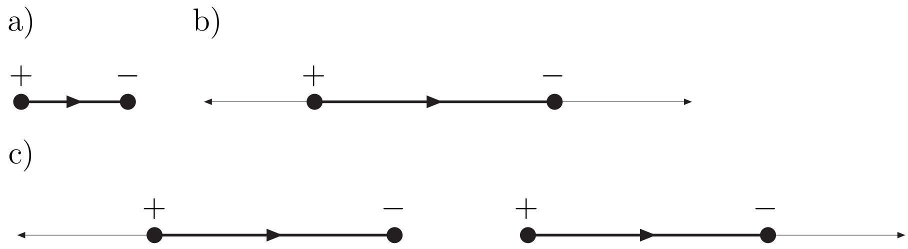

Figure 5: a) Two opposite charges in one dimension, with the field drawn as a thick line with an arrow indicating the direction of the force flux. b) When one of the particles get a kick and the pair get separated, the energy in the field between them increases. The figure is drawn in the CM-system of the particles and the thin arrows indicates the velocities of the particles. c) Eventually another pair of oppositely charged particles can be created.

where the e_i denote the charge of the quark of type i. To a first approximation F_2 only depends on a single variable. From eq. (2) x_{Bj} is a natural choice in this picture. Since x_{Bj} is a ratio of two squared masses the DIS event is to a first approximation described by a dimensionless variable. This is called Bjorken scaling. It turns out, however, that F_2 also has a weak dependence on Q^2 for fixed x_{Bj}. There are two ways a quark may carry the energy fraction x. Either it may have carried it initially, or it may have carried a bigger fraction initially but radiated one or many gluons and thence ended up with a fraction x. With a large Q^2 the photon can resolve more virtual partons, the available phase space for gluon emission is larger, and therefore the Bjorken scaling is violated. Hence $F_2 = F_2(x, Q^2)$. If a parton with momentum fraction x_0 emits a gluon with momentum $(1 - z_1)\hat{P}$ it falls down to the fraction $z_1 x_0$. With many emissions the definition of x_{Bj} in eq. (2) must then be altered to

$$x_{Bj} = \prod_i z_i \cdot x_0. \tag{4}$$

When probing the proton with a photon with a large enough virtuality it can resolve the individual partons. Quantum mechanical interference effects and binding effects can then be neglected and the partons react with the photon as if they were free particles as opposed to the confined particles we know them to be, as described in the next section. This effect is called Asymptotic Freedom and can be derived from QCD. Asymptotic Freedom is a property of the partons that is fundamental in nature and is essential for the parton model.

2.6 The Lund String Fragmentation Model

Even though there have been overwhelming evidence for the quark model to be correct, one has still not observed any single free quarks or indeed any isolated coloured objects in laboratories. Only colourless multi quark or gluon states have been seen in nature. A model describing the transition between coloured quarks and gluons, on the one hand, and the observed colourless hadronic final states, on the other, is needed. The Lund String Fragmentation Model [1] is one such model.

When two electric charges get separated, the electric field between them falls off as one over the square of the distance between the charges. Generally, a Coloumb force in

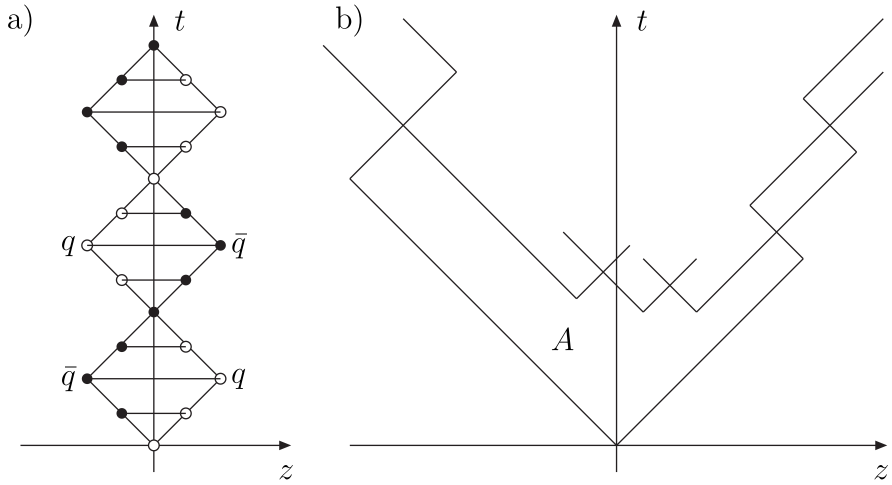

Figure 6: a) A quark and an antiquark in their CM-system. When separated they oscillate through each other in a so called yo-yo mode. b) If the separation becomes large enough the string brakes creating a new quark-antiquark pair.

d dimensions falls off as $r^{-(d-1)}$. We see that in one dimension the force does not fall off, but stays constant, in which case the energy in the field grows linearly with the distance. If we imagine an isolated charge in one dimension, the constant force field would stretch infinitely away from the charge and the energy in the field would hence be infinite. If we had two opposite charges, the forcefield would only exist between them and the energy stored in the field would be proportional to the distance between the two particles. If we enhance the separation, enough energy would be stored in the forcefield to create a pair of oppositely charged particles breaking the field between the charges as in fig. 5.

When separating two oppositely charged particles with a large energy input in a one dimensional system one would obtain many uncharged particle pairs in the final state and *no* isolated charged particles. This is exactly the way the strong force seems to behave. For some reason, it therefore appears that the strong force field only spreads in *one* dimension, in which the colour-charged particles are confined. An explanation for this could be the self-interaction between gluons. It has been demonstrated that a quark-gluon soup can, due to self interaction, get a negative total energy. Since by definition vacuum is the state of lowest energy, vacuum would therefore consist of a quark-gluon soup. Whenever one has to deal with a medium, theoretical predictions get very difficult, but it is generally believed that this quark-gluon soup makes the strongly interacting particles confined. A way to understand a phenomenon is to look for other phenomena showing the same kind of behavior. A phenomenon similar to the strong force confinement is the Meissner effect in superconductors. When a superconductor of type II is put into a magnetic field, the magnetic field lines are compressed into tubes called vortex-lines. For the Meissner effect to be possible a medium is needed, in this case a cloud of bosonic superconducting electron pairs.

In the Lund Model, these tubes are approximated by one-dimensional massless strings where, in the string's rest frame, the energy is uniformly distributed throughout the string according to $\mathrm{d}E = \kappa \mathrm{d}x$. The string tension κ is of the order 1 GeV/fm. When a quark and an antiquark are created, e.g. in an electron-positron annihilation process, and are separated, they are pulled together again, if their energy is low enough, and enter into a so called yo-yo mode as illustrated in fig. 6 a). This may be used as a model of a meson.

If the energy of the quarks is large the quarks will separate enough for the string to break, creating another quark-antiquark pair. The string will continue breaking until all what remains are quark-antiquark pairs in yo-yo modes. What will be obtained in the end is two jets of hadrons in the directions of the original quark and antiquark. It should be noted that this is in the approximation in which the quarks are massless.

When particles with mass are created from the colour-strings, creation in one point is no longer energetically allowed in a classical picture. Instead a semiclassical picture is used where the particles are created by tunneling through a potential barrier as shown in fig. 7 b). Creation of massive particles is thus exponentially suppressed. When massive particles are created there is an ambiguity concerning which particle is created first, as illustrated in fig. 7 a). The world lines of the massive particles are approaching the lines of massless particles asymptotically. Particles may also be created with a four-momentum out of the zt-plane and the mass in fig. 7 must then be replaced by the transverse mass defined by $m_\perp^2 = m^2 + p_\perp^2$. It turns out that the probability for obtaining a specific

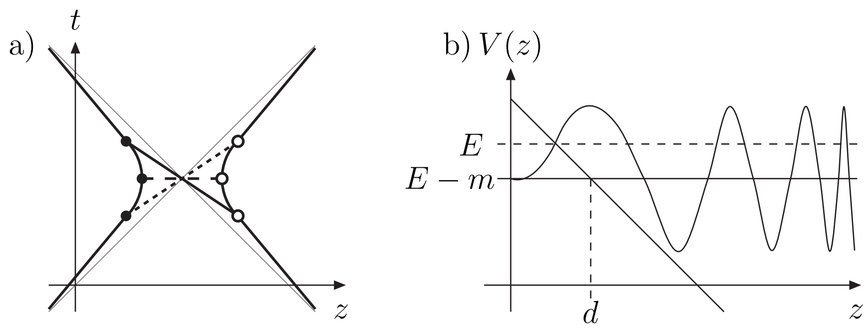

Figure 7: a) Two massive particles are created in a point when the string breaks and are then separated. The system is not Lorenz invariant. If one particle is created first in one Lorenz-system the other may be created first in another. The three lines connecting the quarks illustrates different systems. b) In the Lund Model the creation of massive particles is described by a tunneling through a potential $V(z)$. The wavefunction of one of the particles is also schematically drawn in the plot.

hadronic final state in the Lund model depends on the area A in fig. 6 and is given by the so called Area Law:

$$\mathrm{d}\mathcal{P} \propto e^{-bA} e^{-\frac{1}{2\sigma^2}\sum_j^n m_{\perp j}^2} \delta\left(\sum_{k=0}^{n-1} p_k - p_{tot}\right) \prod_{i=0}^{n-1} N_i \delta(p_i^2 - m_i^2) \mathrm{d}^4 p_i \tag{5}$$

where N_i are mass dependent normalization factors. We see that the suppression of particles with large transverse mass is taken into account.

So far no gluons have been included into the model. A gluon is treated as a kink on a string segment between a quark and an antiquark. The force acting on the gluon through the string is twice the force acting on the quarks. The gluon hadronizes when the string breaks on both sides of the kink, thus creating a jet in which a hadron including the original kink is emitted. If the kink is hard enough it will give rise to a gluon jet. Conventional models built more directly upon perturbative QCD have a problem concerning emission

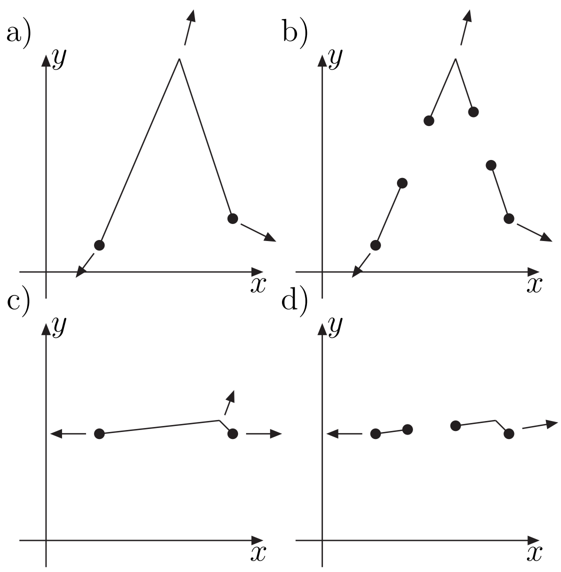

Figure 8: a) The string segment between a quark and an antiquark get a kink. This kink acts as a gluon. b) The string fragmentates into hadrons, the kink gets embedded into one of the hadrons. If the gluon is hard enough it give rise to a third jet. c) A gluon is emitted close to one of the quarks. d) When hadronizing the collinear gluon does not give rise to a jet.

of low-energy gluons. The probability for emitting a soft gluon diverges. In Monte Carlo simulations soft gluons have to be avoided by cut-offs in e.g. $p_\perp$. The models more directly built on perturbative QCD are very sensitive to the cut-off in $p_\perp$, since in those models even soft gluons give rise to gluon-jets. The Lund String Model is not very sensitive to the cut-off. Instead the cut-off is introduced in a natural way. If the gluon is too soft, it does not have enough energy to break the string before it has lost its energy and stopped. In this case, the only contribution from the gluon is a small $p_\perp$ broadening of the two quark-jets. If the string is given a kink very close to one of the quarks there will not be enough energy in the string segment between the gluon and the quark for it to break. The string will then only break on the other side of the gluon and what is obtained is a quark-jet containing the whole string piece between the kink and the quark. In this way the Lund Model is infra-red stable.

The Lund model is a semi-classical model in the sense that it does not include wave-functions and amplitudes, but it contains many quantum mechanical considerations. To make the model fully quantized and still keep the notion of one dimensional strings one would need 26 space-time dimensions (or 10 with some fermionic degrees of freedom) which is not desirable. To perform the quantization in four dimensions one would need to remake some of the assumptions of the model. For example one could allow for a thickness of the strings or let the strings be massive. Considering this, the model works remarkably well.

3 The Colour Dipole Model and the ARIADNE Cascade

When a quark-antiquark pair is produced, e.g. in an e^+e^- annihilation process, and emits gluons the contributions of the two diagrams in figs. 9 a) and b) cannot be distinguished, and the amplitudes of the two diagrams have to be added. A different viewpoint one might take is one in which the quarks form a dipole and when they get separated they radiate dipole emission as illustrated in fig. 9 c). This can be generalized such that the two new dipoles can emit a second softer gluon creating two new dipoles which in turn can emit even softer gluons etc. as in figs. 9 d) and e).

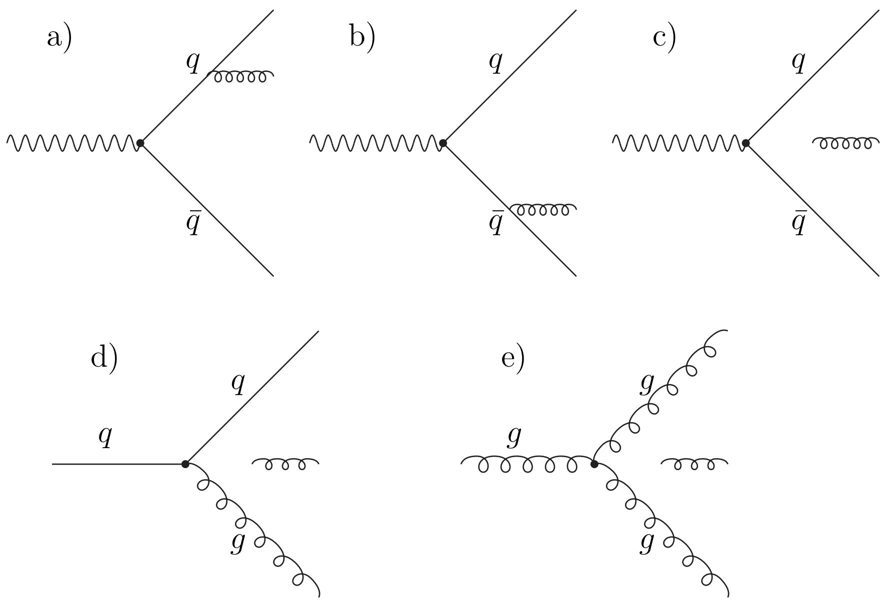

Figure 9: Feynman diagrams for gluon emission from a $q\bar{q}$, qg and a gg dipole. A gluon emitted from one of the quarks in a) or b) can be interpreted as a gluon emitted from the colour dipole created by the separation of the quarks c). The emitted gluons are in turn regarded as parts of dipoles emitting as in d) and e).

3.1 Splitting Functions and Phase-space

If the two partons in the dipole have four-momenta p_1 and p_3, we can define the Lorentz invariant quantity $s \equiv (p_1 + p_3)^2$, which is the square of the center of mass energy of the $q\bar{q}$ system. After the emission, the three partons have the energies $e_i = \frac{1}{2}x_i\sqrt{s}$ in the CM-system of the original dipole, such that the relations $x_1 + x_2 + x_3 = 2$ and $0 \leq x_i \leq 1$ conserve the total energy.

In conventional parton cascades, the probability for an event is approximated by a product of independent emissions, thus omitting all interference effects between emissions. The functions which describe the probability for each independent emission are called “splitting functions”. In the CDM a colour dipole radiates as a unit, which takes into acount the interference from its two colour-charges. The probability for an event is

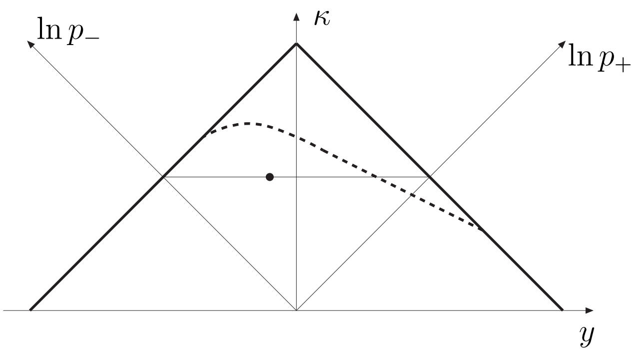

Figure 10: The available phase space for a gluon emitted by a dipole. When a gluon is emitted at the dot, two dipoles are created and can in their turn radiate in the phase-space under the vertical thin line. The dotted curve is the further phase-space restriction when one of the particles in the dipole is extended, as described by eq. (17). Here the extended object carries the larger rapidity.

then approximated by a product of independent emissions from the *dipoles*. Here, the functions describing the probabilities of the splittings of the dipoles are also called "splitting functions". Expressed in the fractions x_i the relevant splitting functions for the three cases in figs. 9 can be written [2]

$$\mathrm{d}P_{q\bar{q}} = \frac{2\alpha_{\mathrm{s}}}{3\pi}\frac{x_1^2 + x_3^2}{(1-x_1)(1-x_3)}\mathrm{d}x_1\mathrm{d}x_3 \tag{6}$$

$$\mathrm{d}P_{qg} = \frac{3\alpha_{\mathrm{s}}}{4\pi}\frac{x_1^2 + x_3^3}{(1-x_1)(1-x_3)}\mathrm{d}x_1\mathrm{d}x_3 \tag{7}$$

$$\mathrm{d}P_{gg} = \frac{3\alpha_{\mathrm{s}}}{4\pi}\frac{x_1^3 + x_3^3}{(1-x_1)(1-x_3)}\mathrm{d}x_1\mathrm{d}x_3 \tag{8}$$

Here partons 1 and 3 emit parton 2. The transverse momentum of the emitted gluon is in the CDM defined by [2]

$$p_\perp^2 = s\cdot(1-x_1)(1-x_3) \tag{9}$$

With this definition the rapidity becomes

$$y \equiv \frac{1}{2}\ln\left(\frac{p_{+,2}}{p_{-,2}}\right) = \frac{1}{2}\ln\left(\frac{1-x_3}{1-x_1}\right). \tag{10}$$

Here the lightcone momenta are defined by

$$p_\pm \;\equiv\; e \pm p_{\mathrm{L}} = p_\perp e^{\pm y}. \tag{11}$$

Expressed in $p_\perp$ and y the splitting functions in eqs.(6) through (8) can be approximated by:

$$\mathrm{d}P_{\mathrm{dip}} \approx \frac{\alpha_0}{\ln\left(\frac{p_\perp^2}{\Lambda_{\mathrm{QCD}}^2}\right)}\frac{\mathrm{d}p_\perp^2}{p_\perp^2}\mathrm{d}y = \alpha_0\frac{\mathrm{d}\kappa}{\kappa}\mathrm{d}y \tag{12}$$

The constant α_0 is defined by the relation $\frac{2\alpha_{\mathrm{s}}}{3\pi} = \frac{\alpha_0}{ln(p_\perp^2/\Lambda_{\mathrm{QCD}}^2)}$ and $\kappa \equiv \ln(p_\perp^2/\Lambda_{\mathrm{QCD}}^2)$. When the gluon gets emitted in the direction such that $p_L > 0$ and when $p_\perp \ll e_2$

$$\begin{aligned} y &\equiv \frac{1}{2}\ln\left(\frac{1+\sqrt{1-p_\perp^2/e_2^2}}{1-\sqrt{1-p_\perp^2/e_2^2}}\right) \approx \frac{1}{2}\ln\left(\frac{4e_2^2}{p_\perp^2}-1\right) \approx \ln\left(\frac{\sqrt{x_2}\sqrt{s}}{p_\perp}\right) \leq \\ &\leq \ln\left(\frac{\sqrt{s}}{p_\perp}\right). \end{aligned} \tag{13}$$

When $p_L < 0$ there is a minus sign in the inequality. This defines a triangle in the κy-plane drawn with thick lines in fig. 10. With the definitions of $p_\pm$ above eq.(13) becomes

$$\begin{aligned} \ln p_+ \leq \ln\sqrt{s}, \qquad & y \geq 0 \\ \ln p_- \leq \ln\sqrt{s}, \qquad & y < 0 \end{aligned} \tag{14}$$

which is nothing but conservation of lightcone momentum.

We note that the phase space can be further narrowed by observing that energy conservation and eqs.(9) and (10) demands

$$1 \geq x_2 = 2 - x_1 - x_3 = \frac{p_\perp}{\sqrt{s}}\left(e^y + e^{-y}\right) \Rightarrow p_\perp \leq \frac{\sqrt{s}}{e^y + e^{-y}}. \tag{15}$$

3.2 Ordered Emissions and Sudakov Form Factors

The colour dipole model has been shown to be a good approximation when the emissions are strongly ordered in $p_\perp$ such that $p_{\perp 1} \gg p_{\perp 2} \gg \ldots$. In ARIADNE the order is taken to be strict but not strong by default as illustrated by the thin vertical line in fig. 10.

Often one wants to draw values in a certain order from a distribution. Say one wants to draw values r_i from a distribution $\mathcal{P}(r)$, where $r > 0$, ordered such that the largest r is drawn first. One can then generate values r_i according to the distribution $\mathcal{P}(r_i)\cdot S(r_i, r_{i-1})$. S is called a Sudakov form factor which gives the probability for *not* obtaining an r in the range where $r_{i-1} < r < r_i$. It has been shown that when all r_i are independent, then $\mathcal{P}(r)$ and the sum of all $\mathcal{P}(r_i)\cdot S(r_i, r_{i-1})$ give exactly the same distribution, but in the latter case the r_i values are ordered such that $r_1 > r_2 > \ldots > r_n$. This implies that to impose the order in $p_\perp$ in the CDM, eq. (12) has to be multiplied by a Sudakov form factor for each dipole given by [2]

$$S(p_\perp^2)_{\text{dip}} = \exp\left(-\int_{p_\perp^2}^{p_{\perp,\max}^2}\int_{y_{\min}(p_\perp'^2)}^{y_{\max}(p_\perp'^2)} \mathrm{d}y'\mathrm{d}p_\perp'^2 P_{\text{dip}}(p_\perp'^2, y')\right). \tag{16}$$

This factor makes sure the gluon with the largest $p_\perp$ is emitted first. In the models where one wants to approximate the strong interactions to a non-interfering chain of events, the order chosen is important since the emission of a gluon changes the colour-flow. The order is also important whenever recoils get considerable. As mentioned above, in the CDM the emissions are ordered in transverse momentum. In many other models the emissions are instead ordered in rapidity y. This is a natural choice since the order in rapidity coincides with the order in colour. In some models, e.g. the DGLAP evolution model, the order in $p_\perp$ and rapidity coincides, whereas in other models, such as BFKL, they do not.

Sudakov form factors can also be used when one wants to impose a cut-off, for example a soft cut-off in $p_\perp$ such that the model does not contain divergences. This is easily accomplished by a Sudakov form factor, all one needs to do is stop generating new values when the cut-off is reached.

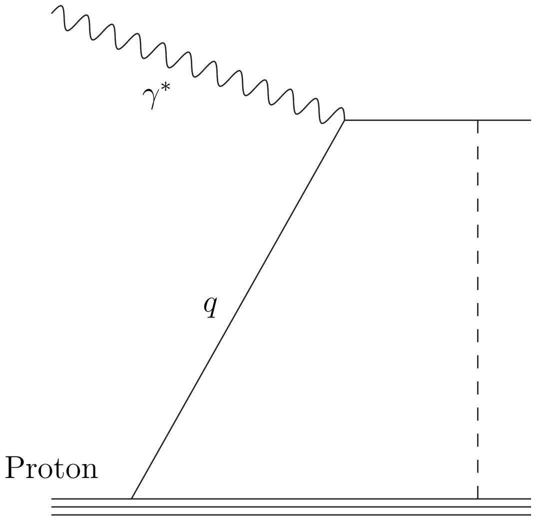

Figure 11: When generating a DIS event in the CDM the initial dipole is formed between the struck quark and the proton remnant. The dipole is shown as the dashed line.

3.3 DIS events in the CDM

When generating DIS events between protons and electrons in the CDM the initial dipole is formed between the struck quark and the proton remnant as shown in fig. 11. This dipole then radiates as described above with one correction. The struck quark is not connected to a point-like particle, but to an extended proton remnant, which needs some special concerns.

When an electromagnetic dipole antenna radiates photons there is a suppression factor proportional to $(2l)^2/\lambda^2$ where l is the effective length of the antenna and λ is the wavelength of the emitted photon. Something similar appears for colour dipole emission when at least one end of the colour dipole does not consist of a point-like particle but of an extended object. In the Lorenz-frame, where the emitted gluon goes out perpendicular to the emitting dipole, the wavelength of the gluon $\lambda = 2\pi/p_\perp$. If the fraction of the extended object participating in the emission is denoted $a(p_\perp)$, eq. (15) must be changed into [3]

$$p_\perp \leq \frac{\sqrt{s} \cdot a(p_\perp)}{e^y a(p_\perp) + e^{-y}}. \tag{17}$$

Here $a(p_\perp) = (\mu/p_\perp)^\alpha$ and α and μ are parameters of the model; α may be regarded as the dimensionality of the remnant, and $1/\mu$ is its transverse extension. An even distribution of the energy of the remainder system over a string, corresponding to $\alpha = 1$, gives good agreement with data. The limit in eq. (17) is schematically drawn as the dashed line in fig. 10, and the maximum is given by [3]

$$p_{\perp,\max} \sim (s\mu^\alpha)^{\frac{1}{\alpha+2}}. \tag{18}$$

The sharp cut-off of eq.(17) can be made less sharp by introducing an exponential suppression in κ of emissions above the dashed line in fig. 10.

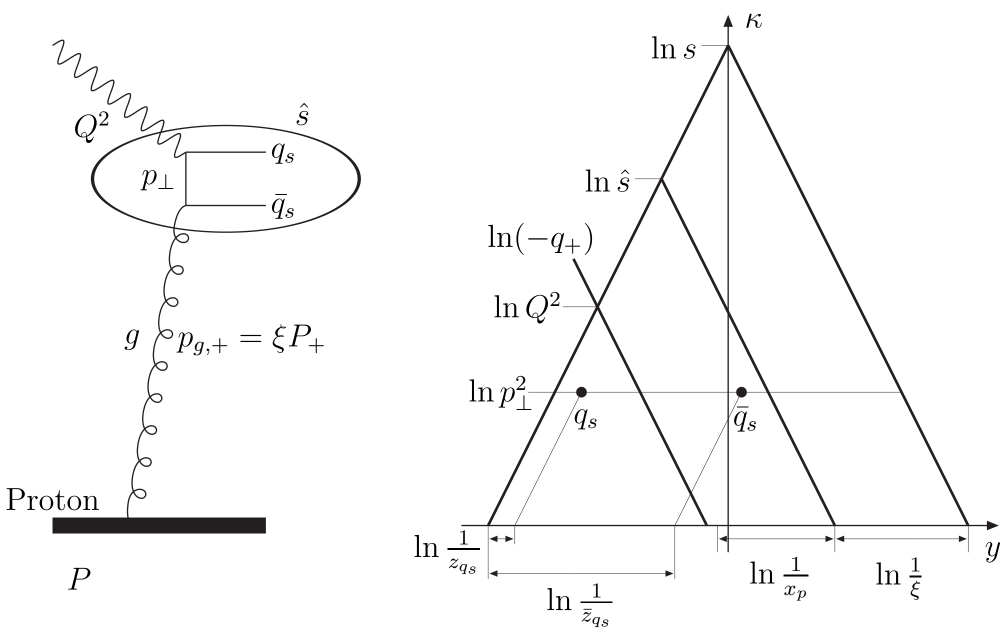

Figure 12: a) A BGF event redrawn with notation. b) a schematic picture of the phase-spaces of a BGF event.

3.4 Sea Quark Interaction and Photon Gluon Fusion

If the struck quark is a seaquark, it is in the CDM connected to two valence quarks in the remnant. The anti-seaquark partner is then assumed to form a meson with the third valence quark. When the struck quark is an anti-seaquark the seaquark partner is assumed to form a baryon with two valence quarks. The hadron in the proton remnant is given a fraction of the original momentum of the proton, as if it was produced in a normal jet in the Lund String Fragmentation Model [1]. The phase space in eq. (17) in the remaining system for gluon emission is then reduced by this fraction.

Fig. 12 a) shows a Boson Gluon Fusion event where a gluon interacts with the photon via a $q\bar{q}$-splitting. In fig. 12 b) the phase-space of the BGF-event is schematically drawn. A gluon is split into a quark-antiquark pair $q_s\bar{q}_s$, where we assume the quark to interact with the photon. The phase space for gluon emissions is further narrowed because the dipoles are connected to extended objects in the proton remnant. The CM-energy of the $q\bar{q}$-subsystem is given by:

$$\hat{s} = (q + p_g)^2 = Q^2(1/x_p - 1). \tag{19}$$

Here $x_p = x/\xi$ is the fraction the struck quark takes of the gluon's p_+. In fig. 12 b) z_q is defined by

$$z_q = \frac{P \cdot p_q}{P \cdot q}. \tag{20}$$

This is the p_--fraction the struck quark takes of the photon.

There are two diagrams to leading order in α_s for BGF-events, and fig. 12 a) only shows one of them. In fig. 13 both are drawn. The matrix-element for the two diagrams is given by [4]

$$M^2 \propto \frac{\alpha_s}{4\pi} \frac{(x_p^2 + (1-x_p)^2)(z_{q_s}^2 + z_{\bar{q}_s}^2)}{(1-z_{q_s})(1-z_{\bar{q}_s})} = \frac{\alpha_s}{4\pi} \frac{(x_p^2 + (1-x_p)^2)(z_{q_s}^2 + (1-z_{q_s})^2)}{z_{q_s}(1-z_{q_s})}. \tag{21}$$

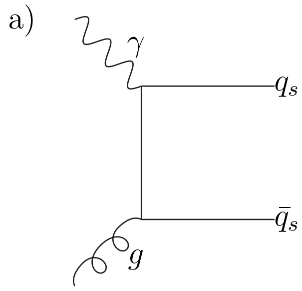

Figure 13: Two Feynman-diagrams interfering.

The probability for a BGF event is then given by [4]

$$\mathcal{P} \propto |M|^2 \frac{g\,(\xi, p_\perp^2)}{f(x, Q^2)} \mathrm{d}x_p \mathrm{d}z_q, \tag{22}$$

where g is the structure function of the gluon in the proton.

When the struck quark is a seaquark in the CDM the initial dipole is formed between the quark and the proton remnant. Eq.(22) can then be interpreted as the probability for emitting the corresponding antiquark as the emission with largest $p_\perp^2$. In ARIADNE two possibilities therefore exist when a seaquark is struck. Either the anti-partner of the struck quark or a gluon is radiated as the emission with largest $p_\perp^2$. Only the former case is treated as BGF. In the latter case the antiquark partner of the struck quark can be emitted with less $p_\perp^2$. The two cases are drawn in fig. 14 a) and b) respectively. A consequence of this scheme is that all radiations closer to the photon in rapidity will also get a larger $p_\perp^2$ than the anti-partner. This is illustrated in the diagram in fig. 14 b) which will only be allowed if the gluon marked g_1 has a larger $p_\perp^2$ than the anti-quark. In other kinds of events, the orders in $p_\perp^2$ and rapidity is uncorrelated in the CDM. ARIADNE's treatment of seaquark-events is therefore somewhat different to how ARIADNE usually treats emissions. This treatment tends to put the partner of the struck sea-quark closer to the proton in rapidity than would be expected. For small x_{Bj} the BGF-diagram in fig. 14 a) will dominate and then this should not have a big influence on the results.

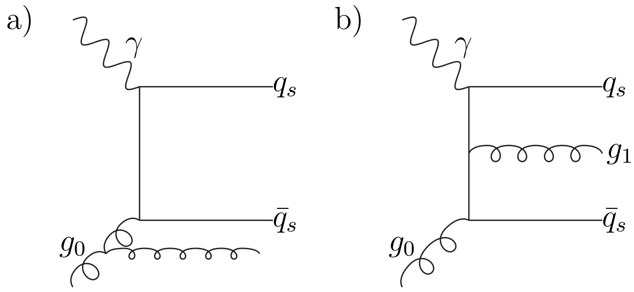

Figure 14: When a seaquark is struck there exist two possibilities in ARIADNE. Either the corresponding antiquark is emitted as the emission with largest $p_\perp^2$ as in a) or one or many gluons are emitted with larger $p_\perp^2$ as in b). The diagram in b) is only allowed in ARIADNE when g_1 has a larger $p_\perp^2$ than $\bar{q}_s$.

3.5 Recoils

When a dipole emits a gluon, transverse momentum is created, which has to be compensated by a recoil to the partons participating in the emission. The colour dipole model assumes that the transverse recoils are distributed in such a way that the disturbance of the colour flow in the neighboring dipoles is minimized. In a qg or a $\bar{q}g$ dipole this implies that the quark should take all the recoil since there is no neighboring dipole on the quark side. For a gg dipole the recoil is distributed according to:

$$\theta = \frac{x_3^2}{x_1^2 + x_3^2}(\pi - \psi), \tag{23}$$

where θ is the polar angle of parton 1 and ψ is the angle between partons 1 and 3.

When one of the emitting particles has a spatial extention, only a fraction of the remnant takes part in the emission and only that part can take the recoil. The string will then get a kink and this kink is treated as a recoil gluon.

The recoil gluon is subject to $p_\perp^2$ ordering in the sense that it will not be emitted if another normal gluon emission between the remnant and the recoil gluon in rapidity gets a larger $p_\perp^2$.

3.6 Mueller's Dipole Model for Heavy Quarks

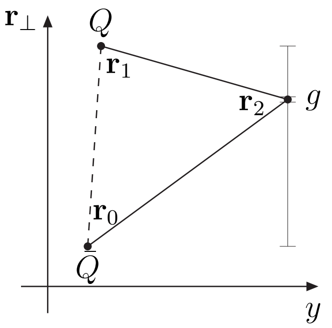

Figure 15: A heavy quark dipole (dashed line) emitting one soft gluon giving rise to two new dipoles (thick lines). The thin lines indicate the size of the dipoles. Here the two-dimensional $\mathbf{r}_\perp$ is symbolically drawn in one dimension. The y on the horizontal axis denotes rapidity.

In this section another colour dipole model, formulated by A.H. Mueller [5], is described. Mueller has chosen not to use $p_\perp$ as a variable for the emitting dipoles, but rather the transverse coordinates $\mathbf{r}_\perp$, which corresponds to a Fourier transform of the momenta of the dipoles. We will look at an onium state consisting of a heavy quark Q and its antiquark partner. Mueller makes the approximation in which a particle does not change it's transverse coordinates after emission. This is valid when the rest-frame of the onium state is moving fast relative to the observer.

Fig. 15 shows two heavy quarks emitting a soft gluon just like in fig. 9c). The lines show the colour dipoles and a dashed line is a dipole which has decayed into two new dipoles and no longer exists. Mueller has shown that for a dipole consisting of two heavy quarks the emissions are described by a splitting function expressed as:

$$\Phi \mathrm{d}y_2 \sim \frac{\bar{\alpha}}{2\pi}\frac{\mathrm{d}^2\mathbf{r}_2 r_{10}^2}{r_{12}^2 r_{20}^2}\mathrm{d}y_2 S(y_1, y_2). \tag{24}$$

Here

$$S(y_1, y_2) \;=\; \exp\left[-\int\int_{y_1}^{y_2} \frac{\bar{\alpha}}{2\pi}\frac{\mathrm{d}^2\mathbf{r}_2 r_{10}^2}{r_{12}^2 r_{20}^2}\mathrm{d}y\right] = \exp\left[-2\bar{\alpha}(y_2 - y_1)\ln\frac{r_{10}}{\rho}\right]. \qquad (25)$$

This is a Sudakov form factor making sure no gluon with $y_1 < y < y_2$ is emitted. Thus the emissions are ordered in rapidity. The ultra violet cut-off, ρ, is taken to be small, introduced such that the integrals do not diverge. This cut-off does not appear in the physics but it is reasonable to use since, if two gluons are very close in space with a very small colour-neutral string-segment in between, the colours of the dipole will not scatter against a target.

When the first emitted gluon is much closer to one of the heavy quarks (say the quark denoted by 1, in fig. 15), than to the other, then $r_{10} \approx r_{20} \gg r_{12}$ and eq. (24) is changed into

$$\Phi \sim \bar{\alpha}\frac{\mathrm{d}^2\mathbf{r}_2}{r_{12}^2}S(y_1, y_2). \qquad (26)$$

We see that the size r_{10} of the dipole which has emitted does not enter. This is also true for subsequent harder emissions, as drawn in fig. 16 a). For the state in fig. 16 a), the multi parton splitting function can be written as

$$\Phi \sim \frac{\mathrm{d}^2\mathbf{r}_2}{r_{21}^2}\ldots\frac{\mathrm{d}^2\mathbf{r}_7}{r_{74}^2}\frac{\mathrm{d}^2\mathbf{r}_8}{r_{87}^2}. \qquad (27)$$

It should be noted that the separation of partons 4 and 7 shows up in eq. (27), even though partons 5 and 6 where emitted by parton 4 before parton 7. The dipole chain connecting partons 8 and 1 should therefore not affect the chain connecting partons 6 and 0, and the two colour-lines emit gluons independently.

In fig. 16 a) partons 1 and 0 have the smallest rapidity and the dipole connecting partons 8 and 7 has the largest rapidity. If the onium state interacts with a photon via the dipole connecting partons 7 and 8, this picture gets very similar to how the BGF-event is treated in the CDM as described in section 3.4. In the CDM there are two dipoles in a BGF-event, each connecting the gluon to a part of the proton remnant. In fig. 16 b) the parts of the remnant are represented by partons 0 and 1. In the CDM those dipoles then emit subsequent softer gluons independently such that in the example in fig. 16 c) the colour-line between 1 and 7 emits gluons 4 and 3 and the line between 0 and 8 emits gluons 6, 5 and 2. In this picture of Mueller dipoles the emissions are less correlated than they are in most other models e.g. in ARIADNE.

The transverse momentum created for every new gluon emitted gives rise to recoil to the particles participating in the emission. It is reasonable to assume that when the particles both lie very far from the emitted particle in coordinate space they share the recoil equally between them, but when one particle lies much closer to the emitted gluon, that particle takes all the recoil alone. With this assumption the recoil of parton 7 in fig. 16 will be given to parton 4, even though partons 5 and 6 were emitted first. This further motivates an assumption in which the two dipole chains are independent.

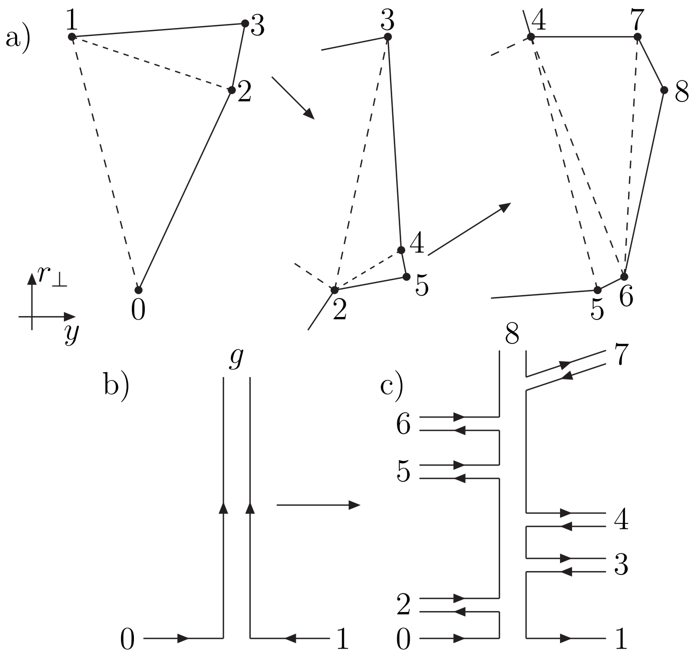

Figure 16: a) The dipole picture for a quark-antiquark pair emitting subsequently harder gluons. The arrows indicate an enhancement of the picture. In b) and c) the same picture as in a) is drawn as a BGF event where the dipole between partons 7 and 8 interacts with the photon. The arrow-lines indicate the colour flux. The two dipole chains between partons 0 and 8 and between 1 and 7 then emits subsequent softer gluons independently.

4 Results

There exist many models for DIS-events. For the description of many variables, the Colour Dipole Model has been the most successful one. This is remarkable since the CDM contains many elements which cannot be derived from perturbative QCD. Therefore, it is interesting to compare the CDM to other models in order to see how they are connected and therefore better understand the strong interaction.

As described in section 3.4 there is a problem with ARIADNE for seaquark-events. When the struck quark in a DIS event is a seaquark two things may happen. Either the antiquark partner of the struck quark is emitted or a gluon is emitted as the emission with largest $p_\perp^2$. This procedure is different from the way other emissions are treated in the CDM. As described in section 3.4, ARIADNE tends to put the antiquark partner of the struck quark closer to the proton in rapidity space than would be expected.

Another version of ARIADNE, subsequently referred to as 'ARIADNE new', has been introduced. In this version the phase-space in both rapidity and $p_\perp$ is larger for the antiquark partner of the struck seaquark. The version described in section 3.4 is referred to as 'ARIADNE default'.

The object of this section is two-fold. Firstly it is to compare the correlation between the quark and antiquark in seaquark interactions in the two versions of ARIADNE. Secondly it is to compare the $p_\perp$ correlation of emissions from the two colour-lines of the struck gluon. For the correlations between the quark and antiquark I have also made comparisons to experimental data from HERA. For the $p_\perp$ correlations of the emissions there is not yet any appropriate measurements made. Instead I have looked for differences between the two versions of ARIADNE in order for future experiments to determine which version of the model is closer to nature.

For the quark-antiquark correlation we anticipate that the anti-partner of the struck quark will get a larger $p_\perp$ in 'ARIADNE new'. We also expect it to come closer to the photon in rapidity. Conservation of total p_+ then implies that the struck quark comes closer to the proton in the new version.

In conventional models implemented in Monte Carlo programs, the emissions from the colour-line and anticolour-line of the struck gluon are very correlated. As described in section 3.6 about Mueller's dipole model, the colour-lines could also be treated as independent emitters. Comparisons between the two cases would therefore be interesting. In 'ARIADNE new' the two dipole-chains are separated. As is illustrated in fig. 17 a) many gluons may be emitted with larger $p_\perp^2$ than the partner of the struck quark in 'ARIADNE default'. All those gluons are emitted with a rapidity closer to the photon than the antiquark is. They are therefore emitted from the same colour-line and are hence very correlated.

ARIADNE is not a complete event generator and it is dependent upon other programs to handle hard interactions, hadronization and particle decays. Interfaced with those programs ARIADNE handles the QCD cascade process. In this thesis LEPTO [6] handles the hard interactions and the Lund String Fragmentation Model implemented in PYTHIA [7], is used to perform hadronization.

4.1 A Comparison to Experimental Data

The H1 Collaboration has studied $D^{*\pm}$ meson production in Deep Inelastic Scattering between electrons and protons at HERA. They have measured the production in the

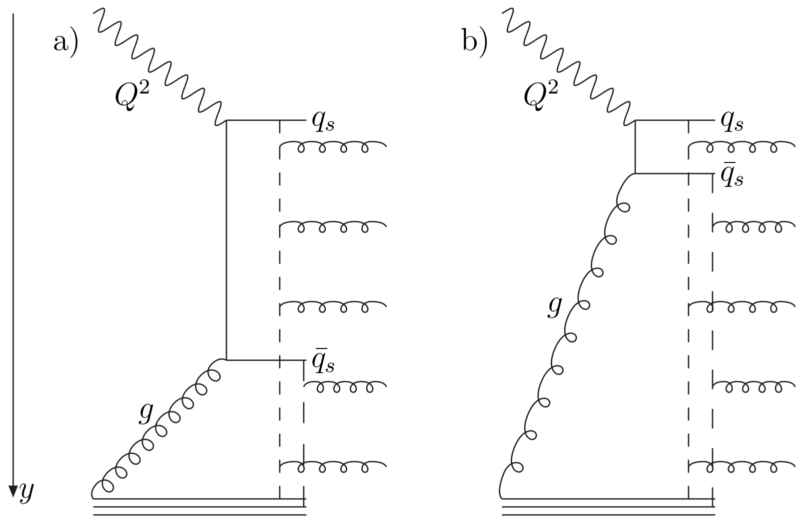

Figure 17: a) In 'ARIADNE default' the antiquark tend to come too far from the photon in rapidity. All gluons harder than the antiquark will end up between the photon and the antiquark. b) In 'ARIADNE new' this is no longer the case. The gluon emissions will also be less correlared in 'ARIADNE new' since they are emitted from both original dipoles at a significant rate.

kinematic region where 1 GeV^2 $< Q^2 <$ 100 GeV^2 and $0.05 < y_{Bj} < 0.7$ where the Bjorken y-variable is defined by

$$y_{Bj} \equiv \frac{Pq}{Pk} = 1 - \frac{E_e'}{E_e} \sin^2\left(\frac{\Theta_e}{2}\right). \tag{28}$$

Thus y_{Bj} is the fraction of the four-momentum of the electron, k, carried by the photon. As before, P is the proton's four-momentum. The last step is valid in the lab-system where E' denotes the energy of the outgoing electron, E_e denotes the energy of the incoming electron and Θ_e is the angle between the two. The study was performed in the lab-frame. The acceptance of the H1-detector were such that $p_{\perp,D^*} > 1.5$ GeV and $|\eta_{D^*}| < 1.5$. This is what the H1-collaboration calls "the visible range". The definition of η is given below. Since $D^{*\pm}$ contains one charm-quark, the major part of the $D^{*\pm}$ will be produced in BGF which is treated as seaquark interactions in the CDM making this a good study for comparisons.

From the discussion above we expect a difference between the two versions of ARIADNE concerning rapidity y of the $D^{*\pm}$. Rapidity is hard to measure, since it includes both the energy and the longitudinal momentum of a particle. Instead, what the H1 Collaboration studied was not the rapidity y but the pseudo-rapidity η defined as

$$\eta \equiv -\ln\left(\tan\left(\frac{\theta}{2}\right)\right). \tag{29}$$

In the lab-system it is easier to obtain η than y, since it only depends on the azimuthal angle θ. The definitions of θ and η are shown in fig. 18. For massless particles η and y are the same.

I have also compared the differential cross-sections with respect to the virtuality Q^2

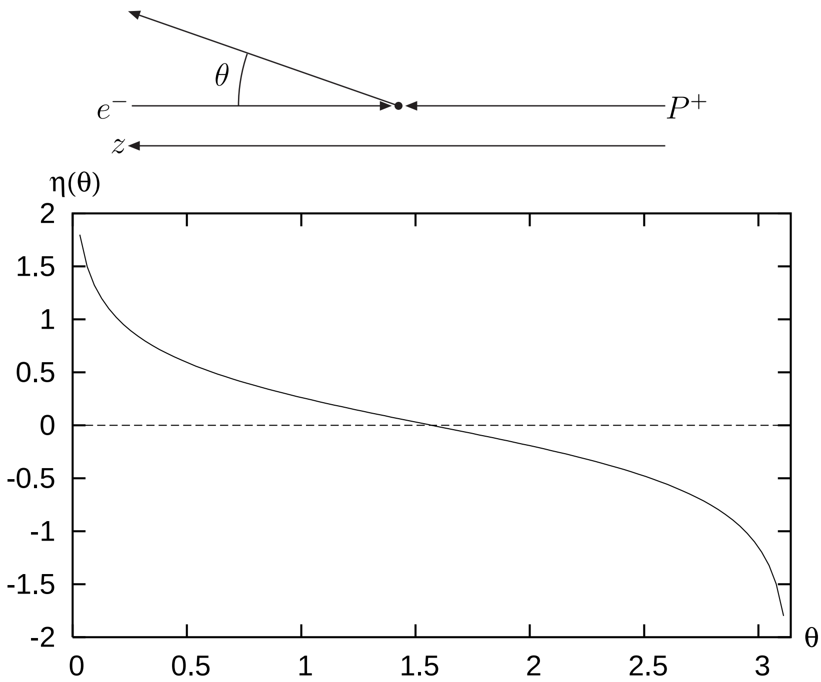

Figure 18: η as a function of θ. We see that positive values of η corresponds to particles going out in the same main direction as the proton, and hadrons with negative η go out in the main direction of the electron.

of the photon, the $p_\perp$ of the $D^{*\pm}$ and to z_{D^*} defined by

$$z_{D^*} = \frac{P \cdot p_{D^*}}{P \cdot q} = \frac{(E - p_z)_{D^*}}{2yE_e}. \tag{30}$$

This is the momentum fraction of the photon just like eq. (20). The last step is only valid in the lab-system. What I have been interested in is the qualitative shape of the curves, not the exact quantitative behavior, which is very dependent upon the structure functions of gluons within the proton. Those are not well known and are not the subject of this thesis.

In the plot where the differential cross-section with respect to $p_\perp$ is shown in fig. 19, the 'ARIADNE default' seems to favor low values of transverse momentum more than the new version. This is expected as discussed above, since other gluons may be emitted with larger $p_\perp$ in the default ARIADNE, reducing the phase-space in $p_\perp$ for the partner of the struck quark. This also has as a consequence that more $D^{*\pm}$ in 'ARIADNE new' end up in the "visible range" for the H1 detector. This will affect all plots.

For small values of Q^2 more $D^{*\pm}$ are produced in 'ARIADNE new' than in the default version. This is the region in Q^2 in which BGF is the dominant process.

The differential cross-section with respect to η in fig. 19, is larger for small η in 'ARIADNE default' than in 'ARIADNE new'. With a bit of imagination, the shape of 'ARIADNE new' seems a bit more similar to the experimental result than 'ARIADNE default'. As shown in fig. 18, small η corresponds to particles in the electron's, and therefore the photon's direction. There the cross-section is expected to be larger in 'ARIADNE new' than in the default version. The result seems to behave the other way around. This can be understood if only the struck (anti)seaquark is found within the acceptance of H1. To see if this was the case I made two new plots, one in which I allow for all values in η and $p_\perp$ and one where I restrict $p_\perp$ as before but still allow for all values in η. Those plots are shown in figs.21 and 22. To make comparisons to figs. 19 and 20 easier they were made in the lab-system. We see that not only does the new version put the anti-partner of the struck quark closer to the photon in rapidity, it also puts the struck quark closer to the proton. This is due to the conservation of total p_+. In figs. 21 and 22 it is evident that the anti-partner of the struck quark in 'ARIADNE default' more often has a $p_\perp$ outside the visible range of the H1 detector compared to 'ARIADNE new'.

No plot in fig. 19 gives a clear enough answer about whether one version of ARIADNE describes the correlation between the heavy quarks better than the other.

In fig. 20 double differential cross-sections are shown. In these plots, the two versions of ARIADNE look more similar. It is therefore not possible to determine which version of ARIADNE is closer to nature in this case either.

Thus, all we can say so far is that there is a clear difference between 'ARIADNE default' and 'ARIADNE new' concerning correlations between quarks and antiquarks in seaquark scattering events, but within the acceptance of the H1 detector it is impossible to determine which one is closer to nature.

4.2 Predictions

As described above, the transverse momenta of the emissions in 'ARIADNE new' are expected to be less correlated than in the default version. This is visualized in fig. 17. No experiments appropriate for comparison has yet been performed. Instead, the object of this section is to find a clear enough signal for future experiments to study. To find a signal I have studied the recoils of the emissions, both with hadrons and with jets clustered as described in [9].

In figure fig. 23 the hardest hadron generated in each event was selected and used as a trigger. The trigger lies in the bin in the plots marked 'Trigger' in fig. 23. I have studied the other hadron's component of $\vec{p}_\perp$ parallel to the trigger's $\vec{p}_\perp$

$$(p_\perp)_{||} = \cos\phi \cdot p_\perp. \tag{31}$$

Here ϕ is the angle between the trigger and the hadron in the xy-plane. Eq.(31) yields both positive and negative results. What is shown in fig. 23 is the ratio of the cross-section for producing a hadron going out in the same hemisphere as the trigger and that for a hadron in the opposite hemisphere, i.e.

$$R(|p_\perp|_{||}) = \frac{\left.\frac{\mathrm{d}\sigma}{\mathrm{d}\left|(p_\perp)_{||}\right|}\right|_{(p_\perp)_{||}\geq\ 0}}{\left.\frac{\mathrm{d}\sigma}{\mathrm{d}\left|(p_\perp)_{||}\right|}\right|_{(p_\perp)_{||}\leq\ 0}}. \tag{32}$$

The data is divided into different bins in η. The $p_\perp$ of the trigger is in the range where 4 GeV $\leq p_{\perp,\text{trigger}} \leq$ 10 GeV for unclustered hadrons and 10 GeV $\leq p_{\perp,\text{trigger}} \leq$ 40 GeV for the jets. To make sure the signal found can be experimentally observed, the simulations were restricted to a total of one million events. The analysis was made in the hadronic center of mass system where the total momentum of the photon and the proton is zero.

What would be expected from the two versions of ARIADNE? In the η-bin of the trigger, the trigger direction should be favored in both versions. This is due to the fact that there is on the order of one jet per unit in η, the trigger is part of that jet and most particles in the bin would therefore travel in the same main direction as the trigger. Sometimes there will be another jet in the same bin. With fig. 17 in mind, this jet could either be from the same colour-line as the first jet in 'ARIADNE new' and then it would pick up the recoil of that jet and go out in the hemisphere opposite to the trigger, or it could have been emitted from the other colour-line in which case it may have any direction and gives no net contribution to the ratio in itself. In 'ARIADNE default' the other jet would often take the recoil of the first and therefore get emitted in the same hemisphere as the trigger. When all this is taken into account, both versions are expected to give a ratio above one in the η-bin of the trigger, but 'ARIADNE new' more so.

In fig. 23 this is really the case when the trigger either is emitted with more energy in the direction of the electron (first plot, first row) or in the direction of the proton (third plot, third row), but in the middle of the range (third plot, middle row) the ratio of 'ARIADNE default' seems to lie just below unity. This may be understood if there are more than two jets in this region taking the recoil of the jet of the trigger hadron. In all three trigger-bins a clear signal was found.

The recoils are expected to end up more often in the bins next to the trigger. In 'ARIADNE new', where the dipoles are separated, this is however expected not to happen as often as in 'ARIADNE default'. In the new version it will only happen when the jet in this bin originated from the same dipole chain as the trigger,

In fig. 23 only one of the bins next to the trigger is shown. Those are the plots in the middle of all three rows. The results in those bins are more or less as expected even though they are very similar for the two versions.

Two bins away from the trigger 'ARIADNE default' will not be very affected by the recoils since it was taken by the jets next to the trigger. In 'ARIADNE new' we still expect the jets coming from these bins to take parts of the recoil from the trigger by a significant rate, lowering the ratio. 'ARIADNE new' is therefore expected to have a lower ratio in these bins.

In fig. 23 this is indeed what we see. It is in these bins the clearest signal is found.

If one wants to construct an experiment to determine which version of the dipole model is closer to nature, the conclusions one may draw from fig. 23 is that one would find the signal in the bins two units in η away from the trigger and in the bins of the trigger.

I have also clustered the hadrons, with the $k_\perp$-clustering algorithm described in [9], and binned in the same way as with the hadrons, only this time I have used a jet as a trigger. The results from this are shown in fig. 24.

With the hadrons clustered into jets we would expect both versions of ARIADNE to give a ratio below unity in the bin of the trigger. When other jets are present in this bin, 'ARIADNE default' is expected to have a lower ratio than 'ARIADNE new', since in the default version the other jets are not expected to be emitted in the same main direction as the trigger-jet. In the bins one and two units in η from the trigger the jets are expected to behave in more or less the same way as the hadrons did. We therefore expect the clearest signal to be found two units in η from the trigger.

In fig. 24 this is close to what is observed. The result is not as clear as it was for the hadrons, though. This could be due to the loss of statistics when the hadrons are clustered into jets.

4.3 Conclusions and Outlook for the Future

The aim of this thesis was to study the dynamics of DIS events at small x_{Bj}. In particular I have studied correllations in heavy quark-antiquark pairs and recoil effects in the gluonic ladder in Boson Gluon Fusion events.

There are many models describing DIS-events. For the description of many observables the Soft Radiation Model, also called the Colour Dipole Model (CDM), as implemented in ARIADNE has provided the best results. The basis for the CDM in DIS events is a dynamical picture of gluon radiation in events, where the virtual photon kicks out a quark from the proton. The gluons are in the model emitted from the colour-separation between the struck quark and the proton remnant. For small x_{Bj}, a significant part of the total cross-section is given by Boson Gluon Fusion events. When BGF was added to the CDM, the details of the implementation was less constrained by the initial dynamical assumptions. The fact that it still provides such a good description of many features of the strong force makes it interesting to investigate the assumptions made, in order to better understand the properties of the strong force. BGF-events have, in a region of phase-space, been treated in a way which is different from what is expected from perturbative QCD. Thus the antiquark partner will be located in rapidity between all gluons with $p_\perp$ higher than the $p_\perp$ of the antiquark, and the proton. This reduces the cross-section both for rapidities close to the photon and for high transverse momentum for the antiquark partner.

In a BGF-event the virtual photon interacts with a gluon in the proton creating a quark antiquark pair. In the CDM the quark and the antiquark are connected to the proton remnant by two colour dipoles. The emissions from these two colour-lines are independent in the model. In most other models, such as DGLAP or BFKL, the recoils are taken up by the virtual gluon link in a gluonic fan-diagram. This makes the $\vec{p}_\perp$-correlations between the gluon-emissions more local in rapidity in those models. Other models, such as Mueller's dipole model, instead imply that the $\vec{p}_\perp$ of the emissions from the two colour-lines might be less correlated. It would therefore be interesting to see if we can investigate the correlations between the two colour-lines in order to see if one description is closer to nature than the other.

For these purposes another version of ARIADNE called 'ARIADNE new' was introduced, in which the antiquark partner is allowed to have a rapidity between the photon and the hardest gluons. In fig. 17 the difference between the two versions is illustrated.

The obvious effect from the imposed modifications concerns the correlations between the quark and antiquark in seaquark events. This effect was studied in section 4.1. In fig. 21 it was clearly seen that the antiquark partner of the struck quark in 'ARIADNE new' is closer to the photon in rapidity. It was also found that the struck quark comes closer to the proton in rapidity. This is due to conservation of total p_+. When comparing figs. 21 and 22 it was realized that the cross-section for high $p_\perp$ for the anti is larger in the new version. When comparing the results from the two versions to experimental data from the H1-detector at HERA, the signal was, however, found to be too small in the acceptance range of the detector for any definite conclusions to be drawn, as shown in figs. 19 and 20. To determine which version of the CDM describes nature better, more experiments are therefore needed.

When looking at fig. 17 another effect from the modification is observed. In 'ARIADNE default' most gluons will be emitted from the same original dipole, whereas in 'ARIADNE new' a significant part of the emissions will originate from each dipole separately. The

$\vec{p}_\perp$ of the emitted gluons will therefore be less correlated in 'ARIADNE new'. We have here found a variable which may provide information about the $\vec{p}_\perp$-correlations of the two colour-lines. When these correlations were studied in section 4.2, a clear signal was found for the two versions of ARIADNE. This is presented in figs. 23 and 24. This signal would be large enough for an experimental determination. Before this, no definite conclusions may be drawn about the nature of $\vec{p}_\perp$-correlations in BGF-events.

We have a need for more experiments, out of curiosity.

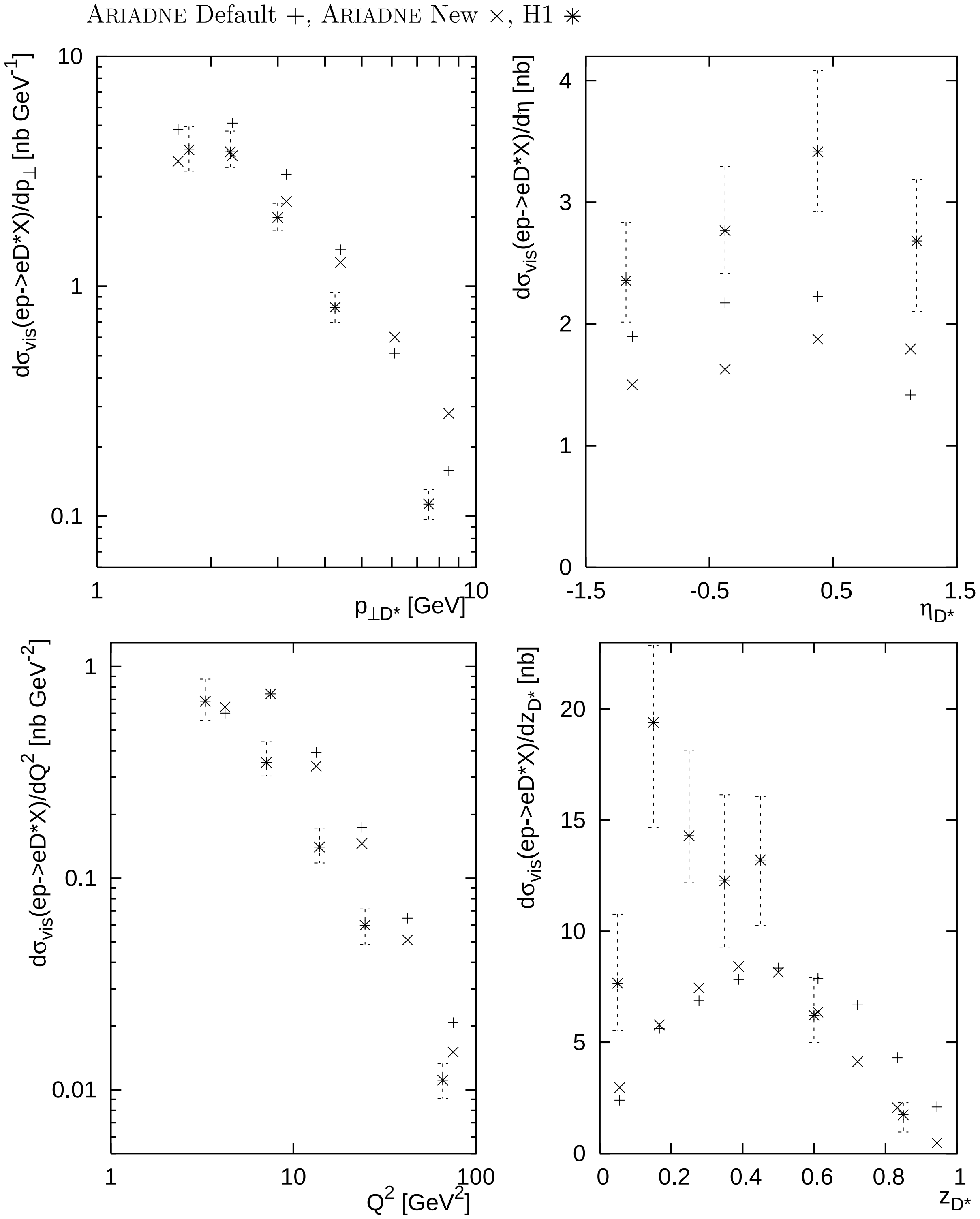

Figure 19: A comparison between ARIADNE run on default and the new ARIADNE with D^* measurements at HERA by the H1 cooperation.

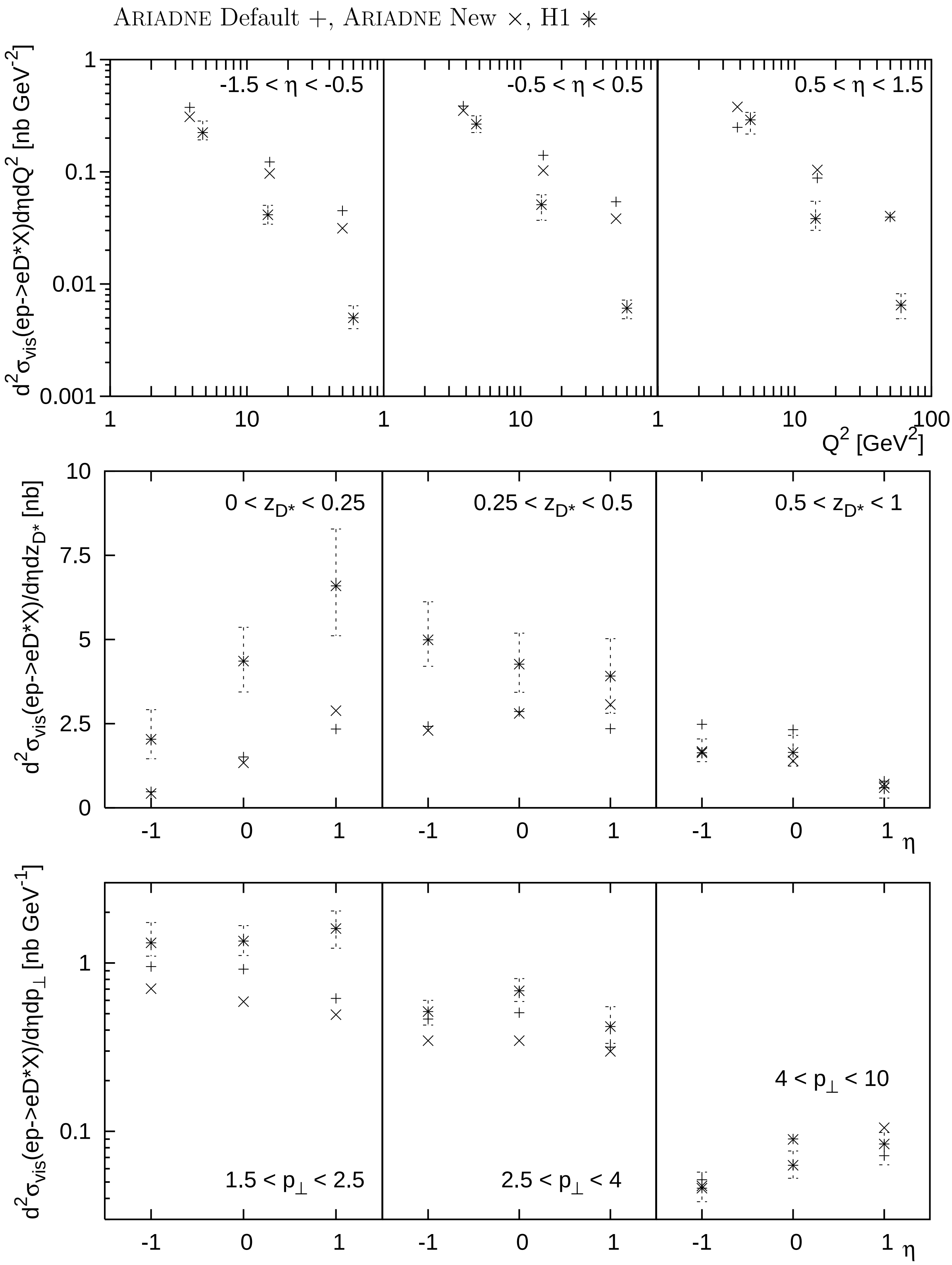

Figure 20: A comparison between ARIADNE run on default and the new ARIADNE with D^* measurements of double differential cross-sections at HERA by the H1 cooperation.

ARIADNE Default +, ARIADNE New ×

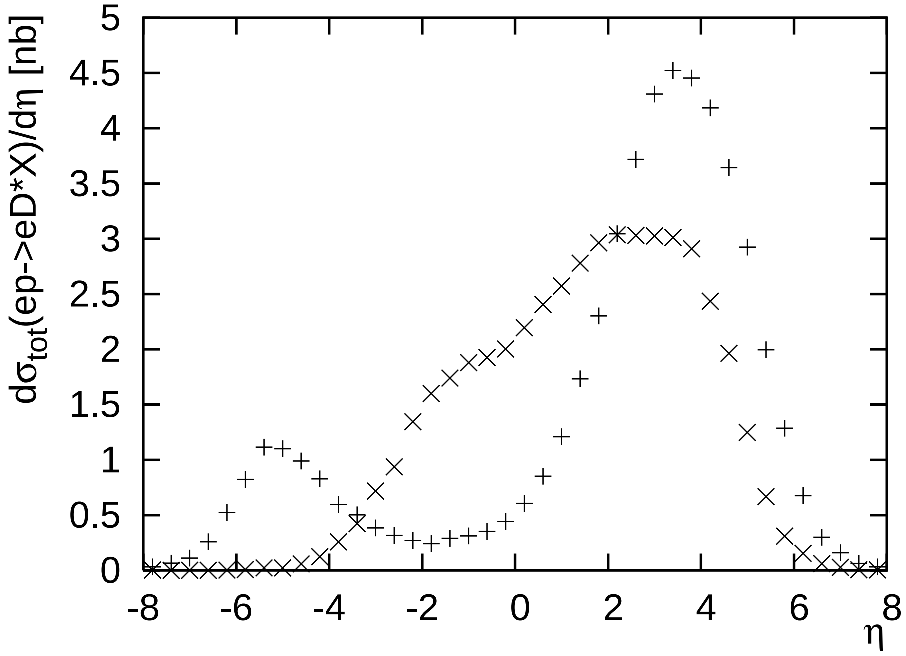

Figure 21: A comparison between the η distributions of $D^{*\pm}$ in the two versions of ARIADNE with no restrictions in η and $p_\perp$ in the lab system.

ARIADNE Default +, ARIADNE New ×

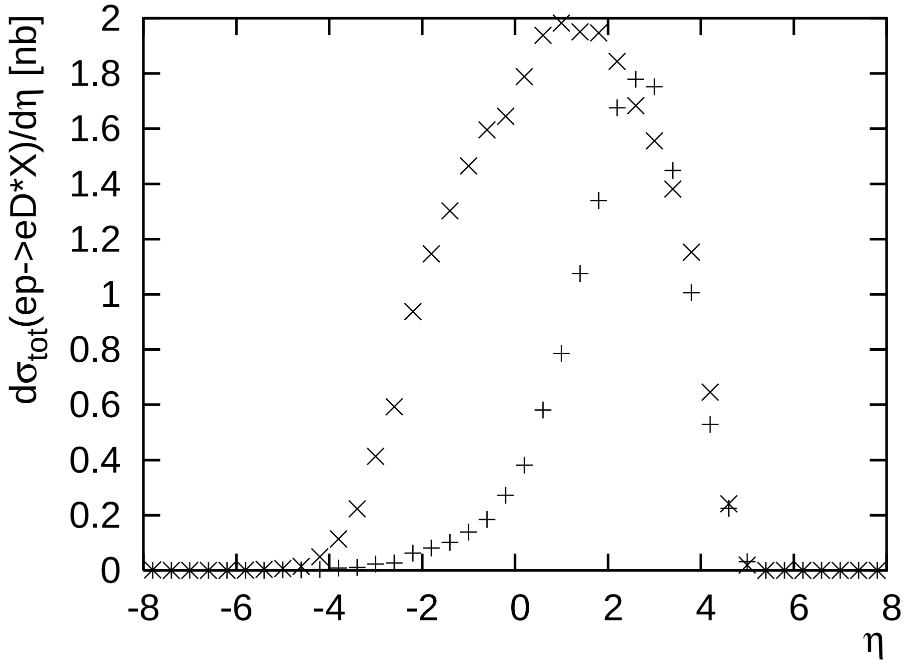

Figure 22: When only $D^{*\pm}$ with transverse momentum above 1.5 GeV is allowed the plot changes.

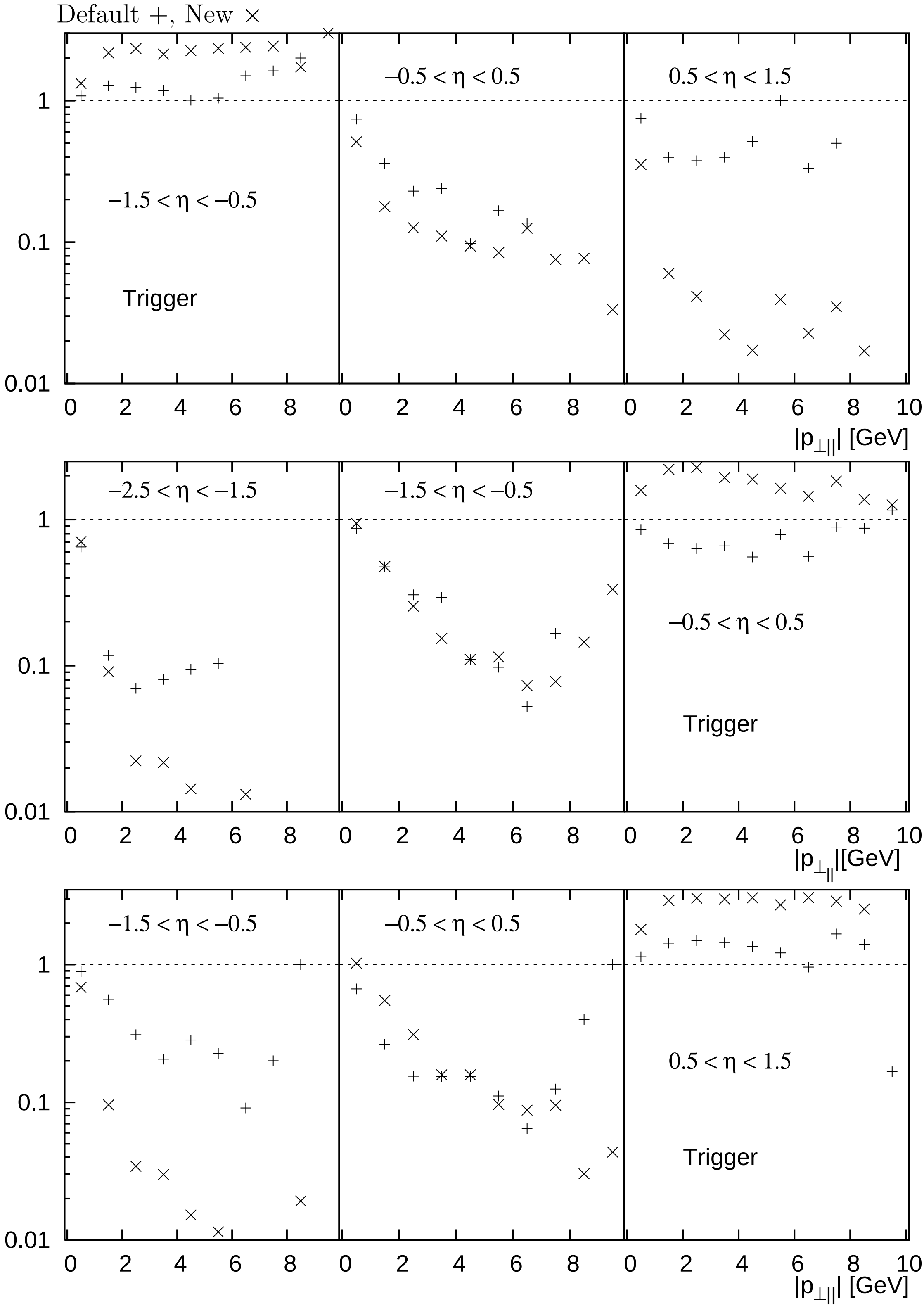

Figure 23: Comparisons between ARIADNE run on default and ARIADNE with the BGF dipoles separated. The trigger lies in the bin of the plot marked with 'Trigger' in each row and in the region where 4 GeV < $p_{\perp,trigger}$ <10 GeV. The diagrams show the ratio defined in eq. (32). The result is in the hadronic center of mass system.

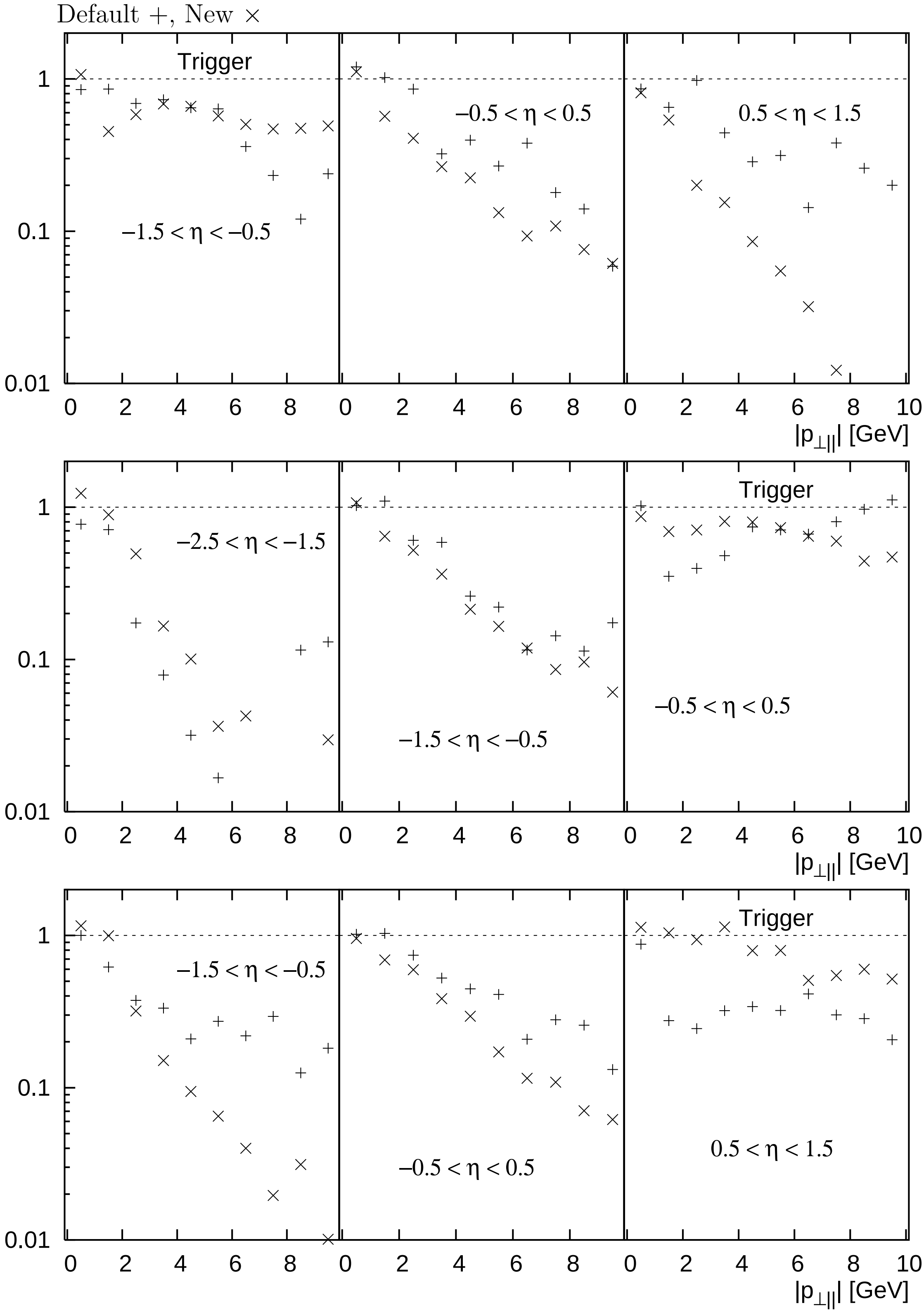

Figure 24: The ratio described in eq. (32) with jets clustered by the algorithm described in [9].

5 Acknowledgments

Gösta Gustafson, Leif Lönnblad and Torbjörn Sjöstrand for always finding time to answer my innumerable questions. All the Master and PhD students which participated at the "Theoretical Physics Informal Student Seminars (THEPISS)" for many a good discussion. The students working at their Master Thesis in Vinterpalatset and elsewhere for the many "bagge" and "fika" breaks. Natanael for always being a source of inspiration.

References

[1] B. Andersson, G. Gustafson, G. Ingelman, T. Sjöstrand "Parton Fragmentation and String Dynamics" *Phys. Rep.* **97** (1983) 31.

[2] L. Lönnblad "ARIADNE version 4: A Program for Simulation of QCD-Cascades Implementing the Colour Dipole Model Revision 12" *Comput. Phys. Commun.* **71** (1992) 15.

[3] B. Andersson, G. Gustafson, L. Lönnblad, U. Pettersson "Coherence Effects In Deep Inelastic Scattering" *Z. Phys.* C **43** (1989) 625.

[4] L. Lönnblad "Gaps and Other Final State Properties in the Dipole Model for Deep Inelastic Scattering" *Z. Phys.* C **65** (1995) 285

[5] A.H. Mueller "Soft gluons in the infinite-momentum wave function and the BFKL pomeron" *Nucl. Phys.* B **415** (1994) 373-385

[6] G. Ingelman, A. Edin, J. Rathsman "LEPTO 6.5 - A Monte Carlo Generator for Deep Inelastic Lepton-Nucleon Scattering" (1996) DESY 96-057

[7] T. Sjöstrand, L. Lönnblad, S. Mrenna, P. Skands "PYTHIA 6.3 Physics and Manual" LU TP 03-38 [hep-ph/0308153]

[8] H1 Collaboration "Measurement of $D^{*\pm}$ Meson Production and F_2^c in Deep- Inelastic Scattering at HERA" [arXiv:hep-ex/0108039 v1 23 Aug 2001]

[9] S. Catani, Y. L. Dokshitzer, M. H. Seymour, B. R. Webber "Longitudinally-Invariant $k_\perp$-Clustering Algorithms for Hadron-Hadron Collisions" *Nucl. Phys.* B **406** (1993) 187